Structures and Stabilities of Alkanethiolate Monolayers on Palladium Clusters As Studied by Gel Permeation Chromatography

Haruno Murayama,[†] Takashi Narushima,[†,‡] Yuichi Negishi,[†,‡] and Tatsuya Tsukuda*[,†,‡]

Research Center for Molecular-Scale Nanoscience, Institute for Molecular Science, Myodaiji, Okazaki 444-8585, Japan, and Department of Photoscience, School of Advanced Sciences, The Graduate University for Advanced Studies, Hayama, Kanagawa 240-0193, Japan

Received: January 26, 2003; In Final Form: January 15, 2004

Palladium clusters protected by a series of *n*-alkanethiolates, Pd:SC_n (SC_n = *n*-$C_nH_{2n+1}S$, *n* = 10, 12, 14, 16, and 18), were prepared by a ligand exchange approach: Pd clusters protected by poly (*N*-vinyl-2-pyrrolidone) (PVP) were transferred from the aqueous phase to the toluene phase containing the thiols. The structures and stabilities of the thiolate monolayers of the Pd:SC_n clusters were investigated by gel permeation chromatography (GPC) together with TEM, XPS, and FT-IR. The thicknesses of the thiolate layers formed on the Pd clusters were evaluated from the differences between the hydrodynamic diameters and core diameters of the Pd:SC_n clusters, determined by GPC and TEM, respectively. The thicknesses thus obtained are in good agreement with the lengths of the corresponding thiolates in the all-trans conformations, illustrating that the alkanethiolates in nearly straight configurations are aligned almost perpendicularly to the core surfaces. Fractionation of the Pd:SC_{18} clusters by GPC yielded a series of the purified samples: the clusters in each fraction are different in their core sizes. The GPC measurements on the Pd:SC_n clusters with small *n* revealed the decomposition of the monolayers through spontaneous etching and their reconstruction by heat treatment in the presence of the free thiols. The mechanism of these processes is discussed. The present study demonstrates that the GPC provides an elemental and versatile means to characterize and purify the monolayer-protected clusters.

1. Introduction

Nanometer-sized metal clusters exhibit size-dependent and size-specific properties that are significantly different from those of the corresponding bulk metal.[1,2] Because of these fascinating properties, metal clusters have gained increasing interests in various fields of nanoscale material science as promising candidates for elementary units of electronic devices, catalysis, sensors, and so on. To manipulate such metal clusters into useful bulk-phase materials without their aggregation, the clusters usually need to be protected by stabilizers such as polymers, surfactants, and ligands.[3] Among the stabilization methods, the protection by the monolayers of thiolates has been one of the most popular passivation routes since the pioneering work by Schiffrin and co-workers in 1994.[4] The resultant molecular assemblies, referred to as monolayer-protected clusters (MPCs), have been the subjects of numerous experimental and theoretical studies.[5−9] As expected, the chemical and interfacial properties of the thiolate ligands on the gold MPCs are analogous in many ways to those of the self-assembled monolayers on flat gold surfaces (2D SAMs).[10−13] On the other hand, one may also anticipate that the monolayer structures of the MPCs are modified to some extent by the structural motifs of the underlying 3D nanocrystallites: the curvatures and populations of defect sites of the 3D surfaces are larger than those of the 2D surfaces. Indeed, it is shown that the coverages of the thiolate ligands on the gold clusters are larger than those on the flat Au(111) surfaces,[14,15] which is ascribed to larger ligand-to-metal ratios on facet edges and vertexes present on the cluster surfaces.[8,9] It is also demonstrated that the alkanethiolate monolayers on the clusters are more liquidlike than the 2D SAMs, due probably to the higher curvatures of the cluster surfaces.[16−18]

The monolayers on the cluster surfaces not merely act as protecting shells but also exert direct influence upon the properties and functions of the MPCs. For example, when one considers applying the MPCs to the fabrication of microelectronic devices, the MPC can be viewed as a nanometer-sized metallic island surrounded by a uniform layer of dielectric media. In such a case, the thickness of the organic layer is an important structural parameter which determines the ability to store electronic charge within the metallic cores (i.e., capacitance of the MPCs).[19−24] The thickness of the organic layer with respect to the core diameter is a key parameter to form self-assembled superlattices of the MPCs.[25] A straightforward method to estimate the thickness of the monolayer, *T*, for a nearly spherical MPC (Figure 1) is to subtract the size of the metal core determined by transmission electron microscope (TEM), d_{core}, from the overall dimension of the MPC, d_{total}:

$$T = (d_{total} - d_{core})/2 \quad (1)$$

A number of methods have been reported so far to determine the d_{total} values. Reetz and co-workers have measured the outer dimensions of surfactant-protected metal particles by using a scanning tunneling microscope (STM).[26] The hydrodynamic Stokes' radii have been estimated on the basis of the diffusion coefficients (Taylor dispersion method) for amine-protected metal particles by Yonezawa et al.[27−30] and for the gold MPCs by Murray and co-workers.[31] More recently, gel permeation

* Corresponding author. Tel: +81-564-55-7351. Fax: +81-564-55-7351. E-mail: tsukuda@ims.ac.jp.
† Institute for Molecular Science.
‡ The Graduate University for Advanced Studies.

10.1021/jp0342125 CCC: $27.50 © 2004 American Chemical Society
Published on Web 02/24/2004

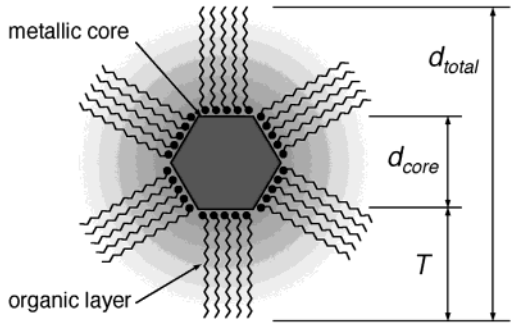

Figure 1. Schematic illustration showing the geometrical parameters of the MPCs; d_{core}, d_{total}, and T represent the size of the metallic core, the overall diameter, and the thickness of the organic layer, respectively.

chromatography (GPC) has been used by Wilcoxon and co-workers to determine the hydrodynamic diameters of the gold MPCs.[32−34]

The stabilities of the monolayers on the metal clusters are also crucial factors to be considered in the fabrication of the MPCs. Ligand place-exchange reactions are one of the key processes to introduce tailor-made functions into the MPCs:

$$x(\mathrm{R'SH}) + (\mathrm{RS})_m\mathrm{MPC} \rightarrow x(\mathrm{RSH}) + (\mathrm{R'S})_x(\mathrm{RS})_{m-x}\mathrm{MPC} \quad (2)$$

where the R′S ligands are incorporated into the RS-monolayers of the MPCs by mixing R′SH and the RS-protected MPCs.[35−38] Recent studies have shown that the exchange reactions of MPCs with thiols and disulfides proceed via associative and dissociative mechanisms, respectively.[37,38] In both cases, the reaction rates are smaller for the MPCs protected by longer chain thiolates, reflecting the higher stabilities of the monolayers. Formation of metal−thiolate complexes, such as Au(I)SR and Pd(II)SR, has been suggested to be involved in the etching reactions of hexanethiolate-protected gold clusters by $C_{12}H_{25}SH$[39] and spontaneous degradation of Pd MPCs,[40,41] although the details of the mechanism have not been clarified yet.

In this study, we investigate the structures and stabilities of alkanethiolate monolayers formed on the Pd clusters by using GPC, TEM, XPS, and FT-IR. Our interest is focused on the chain-length dependences of the structures and stabilities of the thiolate monolayers. The experimental results for the 3D SAMs are also compared with those for the SAMs on the flat Pd surfaces.[42,43] Another important objective of the present study is to demonstrate that the GPC serves as an elemental and versatile tool in purification and characterization of the MPCs.

2. Experimental Section

Chemicals. All the chemicals were commercially available and used without further purification. Palladium chloride ($PdCl_2$), toluene, ethanol, *n*-decanethiols ($C_{10}H_{21}SH$), *n*-dodecanethiols ($C_{12}H_{25}SH$), and *n*-hexadecanethiols ($C_{16}H_{33}SH$) were obtained from Wako Pure Chemical Industries. Poly(*N*-vinyl-2-pyrrolidone) (PVP; $(C_6H_9ON)_n$) with a molecular weight of ca. 40 kDa and *n*-tetradecanethiols ($C_{14}H_{29}SH$) were from Tokyo Kasei Kogyo. *n*-Octadecanethiols ($C_{18}H_{37}SH$) and polystyrene (PS) standards of a GPC grade (M_W 29300, 18700, and 13700) were from Aldrich. The PS standards (M_W 50000, 25000, and 5780) were from Chemco Scientific. The water used in the present study is of a milliQ grade. Hereafter, *n*-alkanethiols (*n*-$C_nH_{2n+1}SH$) are designated as C_nSH.

Preparation of Pd:SC$_n$ Clusters. A two-phase method[44,45] was employed for the preparation of alkanethiolate-protected Pd clusters (Pd:SC_n clusters), which involves ligand exchange reactions of polymer-protected Pd clusters dispersed in aqueous phase. Since the details of the preparation methods of the Pd:SC_n clusters have been reported previously,[44] only a brief description relevant to the present study is given here. The PVP-protected Pd clusters (Pd:PVP) were prepared following the recipe given by Toshima and co-workers.[46,47] The $PdCl_2$ (11.7 mg, 0.066 mmol) powder was put into anhydrous ethanol (50 mL) under vigorous stirring for 24 h. After removing the residue by filtration, the ethanol solution was mixed with 50 mL of water containing 302 mg of PVP. The mixture was refluxed at 363−373 K for 1 h. The color of the mixed solution changed from clear yellow to a transparent dark brown at the beginning of the reflux, due to the formation of Pd clusters via Pd(II) + $CH_3CH_2OH \rightarrow$ Pd(0) + $CH_3CHO + 2H^+$.[46,47] After removing all the water−ethanol solvent by a rotary evaporator, an aqueous solution of the PVP-protected Pd clusters was obtained by redissolving the residue into 100 mL of pure water. The core size of the Pd:PVP clusters thus prepared is determined by TEM measurements to be 2.6 ± 0.5 nm, which is consistent with the previous studies.[46,47] To the hydrosol (20 mL) of the Pd:PVP clusters, the toluene solution (1 mM, 20 mL) of *n*-alkanethiol (C_nSH; n = 10, 12, 14, 16, and 18) was added to form two immiscible layers. The mixture was heated to 363−373 K under stirring for 30 min. The brown color of the Pd clusters was completely transferred from the aqueous layer to the organic layer without any formation of floccules except for the case of $C_{10}SH$. The organic phase was dried over anhydrous $CaCl_2$ for several hours and then filtered. To remove free thiols remained in the toluene phase, the black material obtained by solvent evaporation was precipitated in methanol and the supernatant was discarded. The solvents used in the above procedure are degassed by freeze−pump−thaw cycles before use, and the preparation was conducted under nitrogen atmosphere.

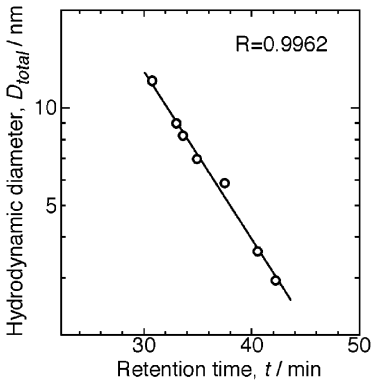

Figure 2. Universal standard curve for the W253 × 2 columns obtained by using the polystyrene standards.

Gel Permeation Chromatography (GPC). We used a recycling preparative HPLC system (LC-908, Japan Analytical Industry Co., Ltd) equipped with two JAIGEL-W253 columns in series. The upper limit of size fractionation, *total exclusion limit*, for the W253 column is 5×10^4. The eluent was toluene, and the flow rate was set to be 3.5 mL/min. The UV−vis absorbance detector was operated at 290 nm. It is well established that the elution times of molecules are governed solely by the hydrodynamic sizes when the affinity between the molecules and the porous micro gels in the column is negligibly small. The calibration curve from which the hydrodynamic diameter was evaluated was obtained by using the monodisperse polystyrene standards (Figure 2): the hydrodynamic diameters of the polystyrenes are given by $(3M\eta/10\pi N)^{1/3}$ on the assumption that they can be viewed as spheres, where M, η, and N represent the molecular weight and viscosity of

the polymer and Avogadro number, respectively.[48] The least-squares fits to the data give the following conversion equation for the W253 × 2 system:

$$d_{\text{total}}/\text{nm} = 492.7 \exp(-0.1209\ (t/\text{min})) \qquad (3)$$

where t represents the retention time. Equation 3 can be regarded as a universal calibration curve to estimate hydrodynamic diameters of the MPCs, because this relationship does not depend on the molecule used as a reference as demonstrated in ref 32. The clusters with the concentration of less than ca. 50 μM were injected into the columns in a typical operation.

Transmission Electron Microscope (TEM). Bright field TEM images were acquired with a HITACHI H-7500 electron microscope operated at 100 kV. TEM specimens were prepared by dropcasting one or two drops of the sample solutions onto a carbon-coated collodion film supported on a copper grid.

X-ray Photoelectron Spectroscopy (XPS). XPS measurements were made using a Vacuum Generators ESCALAB 220i-XL electron spectrometer. The base pressure in the analyzer was ca. 2×10^{-8} Pa. X-rays from the Mg Kα line at 1253.6 eV (15 kV, 20 mA) were used for excitation. Photoelectrons were collected in the constant analyzer energy mode with a pass energy of 100 eV. The binding energies were corrected by referencing the C(1s) binding energy to 284.6 eV.

Fourier Transform Infrared Spectroscopy (FT-IR). Infrared spectra were recorded on a Shimadzu FTIR-8600PC spectrometer with the resolution of 1 cm^{-1} in the transmission mode by accumulating 100 scans. A thick film of the samples was prepared on a KBr plate by dropcasting the corresponding toluene solutions, which was further dried under air.

UV−vis Optical Spectroscopy. Optical spectra of the Pd:SC_n clusters dispersed in toluene were collected on a HITACHI U-2010 spectrometer.

3. Results and Discussion

3.1. Characterization of Pd:SC_n Clusters. *XPS*. Chemical nature of the Pd:SC_n clusters was examined by using XPS. We present in Figure 3 the Pd(3d), S(2p), and N(1s) regions of the XPS spectra of the Pd:SC_{18} clusters prepared under an oxygen-free condition. The Pd(3d) region is composed of doublet peaks at 335 and 340 eV, corresponding to the $3d_{5/2}$ and $3d_{3/2}$ transitions of Pd(0), respectively (Figure 3a). No photoelectron signals are detected in the N(1s) region (Figure 3c), whereas the S(2p) region consists of an unresolved doublet peak at 162 eV associated with the $2p_{3/2}$ and $2p_{1/2}$ transitions of thiolate species (RS^-) bound to the underlying Pd clusters (Figure 3b).[43] These results confirm that the PVP polymers are replaced completely by the thiolates during the phase transfer. Also shown in Figure 3 are the XPS data of the Pd:SC_{18} clusters prepared under ambient air. The comparison indicates that neither the Pd cores nor the thiolates are oxidized into palladium oxides and sulfonates (RSO_3^-), respectively, during the preparation under air. The Pd:SC_n clusters once prepared are also stable against oxidation upon air exposure which will be described in detail in section 3.3.

TEM. Figure 4 shows representative TEM images of the Pd:SC_n clusters which are prepared from an identical hydrosol of the Pd:PVP clusters as the starting material. The spherical Pd cores of the Pd:SC_n clusters are actually fcc single crystals as revealed by high-resolution TEM and XRD measurements.[44,45] The size distributions of the Pd cores are displayed by histograms in the figure. The average core diameters, d_{core}, of the Pd:SC_n clusters are ca. 2.7 nm with a standard deviation,

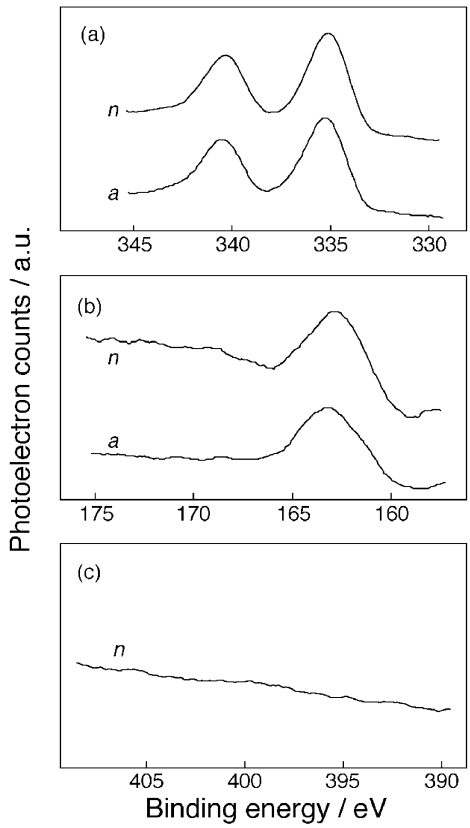

Figure 3. XPS spectra of the Pd:SC_{18} clusters for the core levels of (a) Pd(3d), (b) S(2p), and (c) N(1s). The spectra of the clusters prepared under nitrogen and air are denoted as "*n*" and "*a*", respectively.

σ, of ca. 50% for $n \geq 12$ and 5.3 nm ($\sigma \sim 70\%$) for $n = 10$. An exceptionally large core size for the Pd:SC_{10} clusters is ascribed to the core growth during the washing procedure of the free thiols as demonstrated in Figure 5: the d_{core} value of the Pd:SC_{10} clusters shown in Figure 5a is 2.8 ± 0.7 nm. This phenomenon, observed *only* for the Pd:SC_{10} clusters, can be explained in terms of the instability of the monolayer against desorption: the $C_{10}S$ thiolates are easily detached from the Pd cores due probably to small van der Waals (vdW) interaction between the chains so that the resulting metastable clusters tend to aggregate into larger particles. We observed semi-regular ordering of the Pd cores in some areas of TEM images for $n \geq 12$ (Figures 4a−d). Typical face-to-face spacing is smaller than twice the thiolate's length in the all-trans conformation (see Table 1 in section 3. 2) as observed in 2D superlattices of MPCs, which has been attributed to interdigitation of alkyl chains of neighboring particles.[8,16−18,25,49,50] This assembling behavior of the Pd:SC_n clusters strongly suggests formation of the thiolate monolayers on the Pd cores.

GPC. The transmittances, defined as the survival rates of the Pd:SC_n clusters for elution through the W253 × 2 columns, were obtained on the basis of the absorption spectra and plotted as a function of n in Figure 6. Apparently the transmittance depends heavily on the chain length: ca. 80% of the Pd:SC_n clusters with $n = 18$ and 16 are eluted from the columns, whereas the most of the Pd:SC_n clusters with $n = 12$ and 10 are trapped in the column. Since the injection of the Pd:SC_n clusters with $n \leq 12$ results in a serious contamination of the columns, the GPC results presented hereafter are concerned mainly with the Pd:SC_n clusters with $n \geq 14$. The d_{total} values of the Pd:SC_n clusters ($n \geq 14$) were evaluated on the basis of the GPC data collected with the use of the W253 × 2 columns. Figure 7 shows the chromatograms of the Pd:SC_n clusters whose

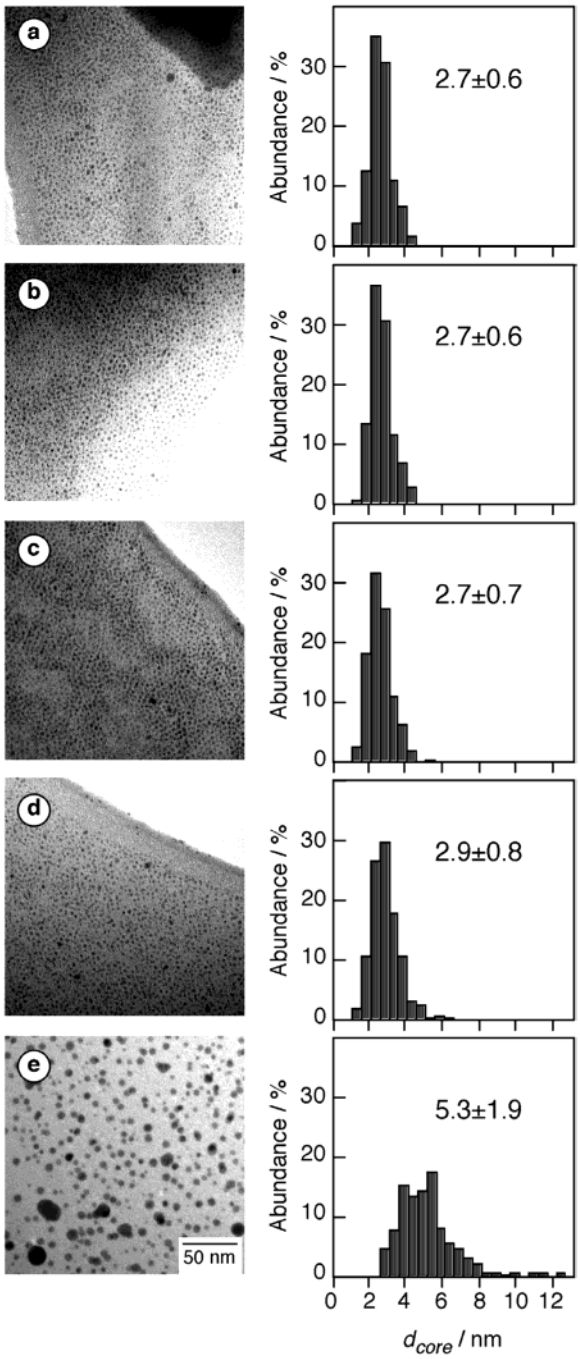

Figure 4. TEM micrographs of the Pd:SC_n clusters: n = (a) 18, (b) 16, (c) 14, (d) 12, and (e) 10. The size distributions of the Pd cores are shown by histograms.

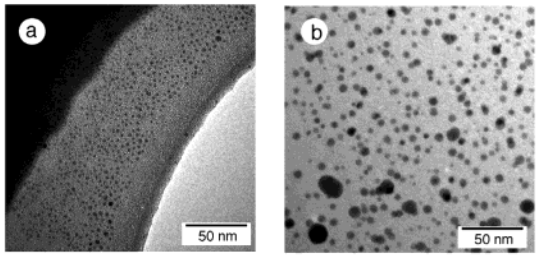

Figure 5. TEM images of Pd:SC_{10} clusters (a) before and (b) after the removal of the excess thiols from the solvents.

TEM images are displayed in Figure 4. The upper abscissa of Figure 7 represents the hydrodynamic diameter derived from eq 3. There appears a series of the GPC peaks in the size regimes larger than the corresponding d_{core} values indicated by the downward arrows in the figure. The d_{total} values of the Pd:SC_n clusters with $n \geq 14$ derived from the elution times are reproducible within the accuracy of ±0.1 nm.

TABLE 1: Summary of the Structural Parameters of the Pd:SC_n Clusters Determined by TEM and GPC Measurements

n	d_{total}/nm[a]	d_{core}/nm[b]	T/nm[c]	T_{free}/nm[d]
18	7.6	2.7 (1.2)	2.5	2.54
16	7.2	2.7 (1.2)	2.3	2.28
14	6.6	2.7 (1.4)	2.0	2.03

[a] From Figure 7. [b] From Figure 4. Numbers in the parenthesis represent the standard deviations. [c] Calculated by eq 1. [d] Obtained from ref 49.

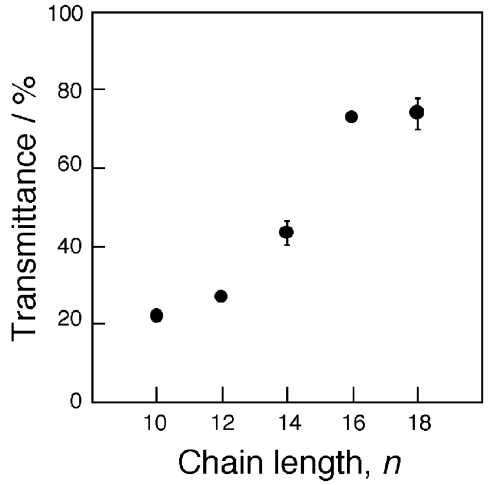

Figure 6. Transmittance of the Pd:SC_n clusters through the W253 × 2 columns as a function of n. The error bars shown for n = 14 and 18 represent the standard deviations of three independent measurements.

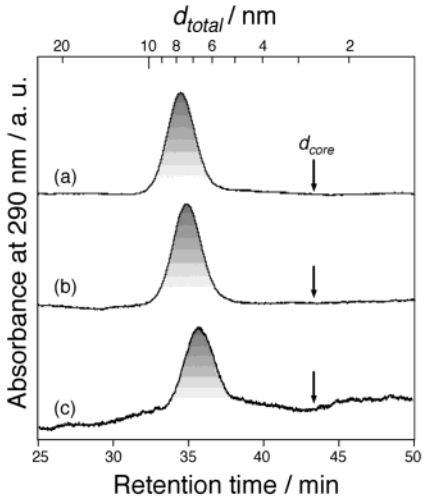

Figure 7. GPC profiles of the Pd:SC_n clusters: n = (a) 18, (b) 16, and (c) 14. The upper abscissa represents the hydrodynamic diameter derived from eq 3. The downward arrows indicate the d_{core} values, determined from Figure 4.

3.2. Structures of Thiolate Monolayers of Pd:SC_n Clusters. Here we summarize in Table 1 the structural parameters of the clusters determined in the previous section. The thicknesses of the monolayers, T, are estimated by using eq 1 on the assumption that uniform layers of the thiolates are formed on the spherical Pd cores. Also listed in Table 1 are the lengths of the alkanethiolate molecules in the straight-chain configurations,

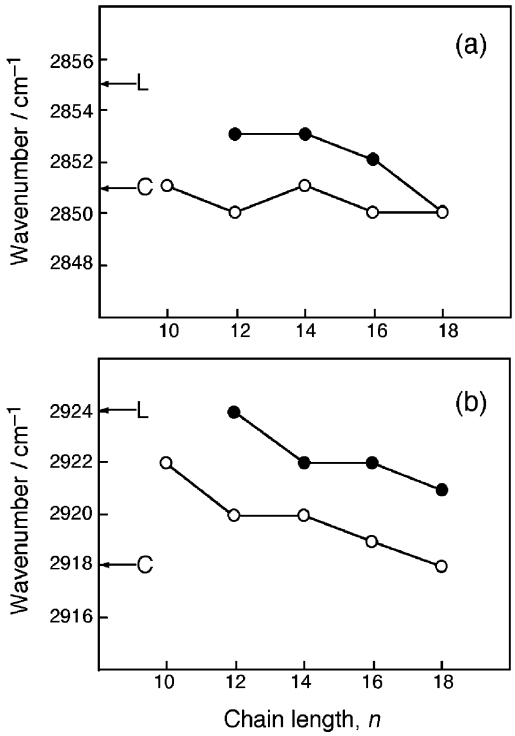

Figure 8. Plots of the vibrational frequencies for the (a) symmetric and (b) antisymmetric CH_2 stretching modes of the thiolates as a function of the chain length, *n*. The data for the Pd clusters and 2-D surface[42,43] are shown by closed and open circles, respectively. The arrows indicated by "L" and "C" represent the frequencies for the liquid state of C_8SH and crystalline state of $C_{22}SH$, respectively.[51]

T_{free}, given by an empirical formula, $T_{free}/nm = 0.25 + 0.127n$, where *n* represents the number of the carbon atoms of the alkyl chains.[49] Table 1 shows that the *T* values are in good agreement with the corresponding T_{free} values and increase almost linearly with the alkyl chain length. These findings provide a plausible model for the structures of the Pd:SC_n clusters: the alkanethiolates in nearly straight configurations are aligned almost perpendicularly to the core surface forming bundles of the alkyl chains. To obtain further information on the monolayer structure, the conformations of the alkyl chains have been investigated by monitoring the frequencies of the CH_2 stretching modes with the use of FT-IR spectroscopy: it is well established that the symmetric (d^+) and antisymmetric (d^-) CH_2 stretching modes of the crystalline SAMs of alkanethiolates on gold surfaces or clusters lie at ca. 2850 cm^{-1} and ca. 2920 cm^{-1}, respectively, and that their frequencies increase as the SAM structure becomes more liquidlike.[5,14,16−18,51,52] In Figure 8, we plot the peak positions for the d^+ and d^- stretching modes of the alkanethiolates on the Pd clusters as a function of the chain length, *n*. The CH_2 stretching frequencies decrease with *n*, showing the increase in the population of the trans conformations in the alkyl chains. This trend can well be explained in terms of larger vdW attractive forces between the longer alkyl chains. The comparison between Figures 6 and 8 suggests that the trasnmittance of the MPCs through the columns is closely correlated with structures of the monolayers. The positive correlation was confirmed by the fact that the d^+ and d^- stretching modes of the Pd:SC_{14} clusters eluted from the columns are shifted to 2851 and 2921 cm^{-1}, respectively: the monolayers of the eluted clusters are on average more solidlike than those of the as-prepared clusters. Therefore, we conclude that only the clusters having highly ordered monolayers can survive through the column due to their negligibly small interaction with the porous microgels in the columns.

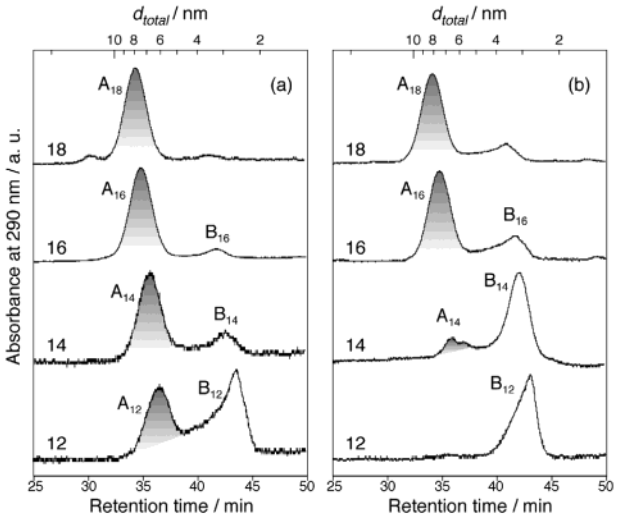

Figure 9. Chromatograms of the Pd:SC_n clusters stored at ambient conditions in (a) toluene and (b) toluene solutions of C_nSH with the concentration of 10 mM. The intensities of the peaks are scaled arbitrarily. The peaks associated with the MPCs (A_n) are shaded.

It is interesting here to compare the structures of the alkanethiolate SAMs on the Pd clusters (3D SAMs) with those on the 2D SAMs reported recently by Whitesides and co-workers.[42,43] The thicknesses of the 2D SAMs have been determined by ellipsometry to be 2.6, 2.3, and 1.9 nm for $n =$ 18, 16, and 14, respectively.[42,43] These values agree with our data for the 3D SAMs (Table 1) within the experimental uncertainty, indicating similar morphologies for the 2D and 3D SAMs. However, the vibrational frequencies of the CH_2 stretching modes of the 3D SAMs are apparently higher than those of the corresponding 2D SAMs (Figure 8). This result indicates that the 3D SAMs contain a higher density of gauche defects than the 2D SAMs, which is due to the reduction of van der Waals attractive forces between the neighboring alkyl chains. Weaker interaction between the alkyl chains of the thiolates on the 3D crystal is ascribed to (1) low density of the alkyl chains at the outermost region associated with large curvature of the underlying 3D clusters and/or (2) higher density of facet edges and vertexes present on the cluster surfaces (see Figure 1).[16−18]

3.3. Stability of Thiolate Monolayers of Pd:SC_n Clusters. *Reactions.* Recently, the degradation of the Pd MPCs has been observed through optical spectroscopy and TEM measurements.[40,41] Chen and co-workers have reported that the Pd:SC_6 clusters eventually decomposed into extremely fine Pd clusters and/or reoxidized into ionic solutions when the solution is stirred under ambient conditions for 90 min.[40] Murray and co-workers have concluded that Pd:SC_n ($n = 6$ and 12) clusters formed in the presence of an excess amount of RSH revert in time to Pd(II) thiolate complexes.[41] To elucidate the detailed mechanism, we followed up the degradation processes of the Pd:SC_n clusters with the use of GPC technique. Figure 9a represents the chromatograms of the Pd:SC_n clusters which were stored for 100 hr in toluene under ambient air. There appears a new series of peaks denoted as B_n in addition to the series A_n associated with the MPCs (Figure 7). The B_n peaks become more prominent with decrease in the chain length *n*. These results indicate that the MPCs spontaneously decompose into smaller species associated with B_n and that the decomposition proceeds faster in smaller *n*. The species associated with B_n are composed of the corresponding alkanethiolates since their hydrodynamic diameters are dependent on the chain length *n*. The optical

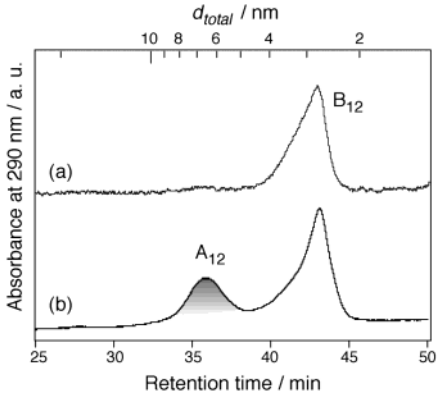

Figure 10. Chromatograms of the Pd:SC_{12} clusters stored for 400 h in toluene solutions of $C_{12}SH$: (a) before and (b) after the incubation at ca. 370 K for 4 h in the presence of the free $C_{12}SH$. The ordinates for the profiles are referenced to each other.

absorption spectrum of the B_n fraction exhibits an onset at ca. 600 nm and peaks at 320 and 410 nm. On the basis of these results, we infer that the Pd(II) thiolate complexes[53] are the most plausible species responsible for the B_n as suggested by Murray and co-workers.[41] Further investigation to fully characterize the chemical identity of B_n is beyond the scope of the present study. Also shown in Figure 9b are the chromatograms of the Pd:SC_n clusters, which were allowed to react with the free C_nSH thiols (10 mM) for 100 hr. It is evident that the degradation of MPCs into the Pd thiolates is accelerated by the presence of free thiols. Note that the intensities of the A_n peaks are related not only to the concentration of the MPCs but also to the degree of structural order of the monolayers as described in section 3.2. For example, although the A_{12} peak is absent in Figure 9b, the presence of the Pd nanoparticles (ca. 3 nm) was evidenced by optical spectroscopy and TEM observation. Thus the exposure of the MPCs with the free thiols facilitates the formation of the small Pd thiolates (etching) and disarray of the monolayer structures of the MPCs. On the other hand, we noticed that the well-ordered monolayers are reconstructed by incubation of the clusters in the presence of the free thiols. Figure 10 shows that the peak A_{12} is recovered after the refluxing the toluene dispersion of the decomposed clusters containing free $C_{12}SH$: the intensity of the B_{12} peak is unchanged after the treatment.

On the basis of these findings, we propose the following scheme for the chemical processes involved in the monolayers of the Pd:SC_n ($n \leq 16$) clusters (Scheme 1). The short-chain thiolates with $n \leq 16$ tend to be detached from the Pd cores in the form of Pd thiolate complexes (step (i)). This spontaneous dissociation probably occurs preferentially at vertex and edge sites of the underlying Pd nano-crystallites, as has been pointed out in the place-exchange reactions.[37] The free thiols, if present in the solvent, can further act as etchants against the vertexes and edges of the Pd clusters where the packing density of the monolayer is lowered due to the self-dissociation (step (ii)). The monolayers of the resulting clusters become disordered, and as a result the clusters cannot be eluted from the columns. The reconstruction of well-ordered monolayers by heat treatment may result from the effect of annealing on lateral organization of the thiolates[43] as well as on the Pd core structures (step (iii)). These degradations of the Pd:SC_n clusters into the Pd thiolate complexes described here (steps (i) and (ii)) are essentially the same as those reported by the groups of Chen[40] and Murray;[41] however, our clusters dissociate so slowly that the decomposition can hardly be recognized through conventional measurements such as TEM and optical spectroscopy. The origin of such

SCHEME 1: Spontaneous Degradation and Thermally Induced Reconstruction of the Monolayers of the Pd:SC_n Clusters

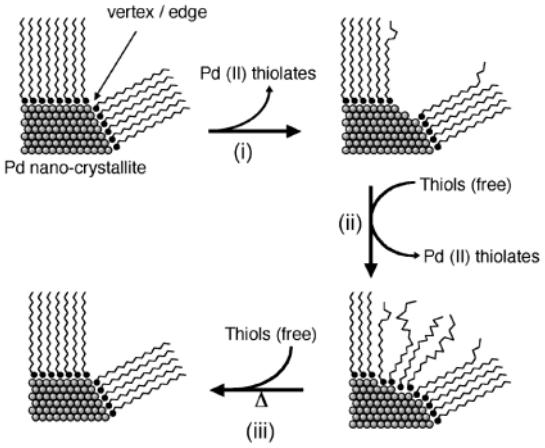

difference probably lies in the preparative conditions of the clusters: the monolayers we prepared at high-temperature are more stable than those prepared by Chen[40] and Murray[41] at ambient temperature. This inference is supported by the observation that the Pd:SC_n clusters prepared by the ligand exchange at room-temperature decomposed much faster than those shown in Figure 9.

Oxidation by Air. It has been well documented that the SAMs of thiolate (RS^-) on 2D metal surfaces are oxidized to sulfinates (RSO_2^-) and/or sulfonates (RSO_3^-) upon prolonged exposure to air.[54−58] While the mechanism of the oxidation process has been the subject of some debate, the ozone present in ambient air or formed by UV light irradiation is believed to act as the primary oxidant. Whitesides and co-workers have recently demonstrated that the $C_{16}S-$SAM on the Pd surface exposed to ozone-free air is "completely" oxidized into alkylsulfonates within 120 h; the XPS peaks at ca. 163 eV due to the Pd−S mixed interface layer and thiolate are taken over by new peaks at ca. 169 eV due to the sulfonate and sulfate.[43] For a comparison purpose, thin films of the Pd:SC_n clusters prepared by dropcasting the toluene dispersions onto copper substrates are allowed to stand for 120 h in the dark at ambient condition. The XPS spectra of the films stored under air and nitrogen are compared in Figure 11. The spectra do not show any appreciable sign of oxidation except for the $C_{12}S$ thiolates, where a small hump is discernible at 169 eV (Figure 11a). Contrary to expectations from the discussion in the previous section, these results indicate that the 3D SAMs are more stable than the 2D SAMs against oxidation by air. The origin of this counter-intuitive behavior is not clear at present.

3.4. Purification of Pd:SC_{18} Clusters. As demonstrated in Figures 9a and 11, the Pd:SC_{18} clusters stored as a toluene dispersion at ambient conditions are stable against air oxidation and spontaneous degradation. The inherent stability and rigidity of the $C_{18}S$ monolayer motivate us to purify the Pd:SC_{18} clusters with the use of the GPC technique. Then, the clusters associated with the A_{18} peak were fractionated into three portions, F1−3, according to the retention times. The d_{total} and d_{core} values of the clusters contained in each fraction were evaluated on the basis of the chromatograms (Figure 12a) and TEM pictures, respectively. The GPC profiles shown in Figure 12a demonstrate that the d_{total} values are reduced in the order of F1, F2, and F3 and that the dispersions are appreciably improved by the fractionation. The TEM image of the clusters in F2, for example, is shown in Figure 12b, and the core size distribution is

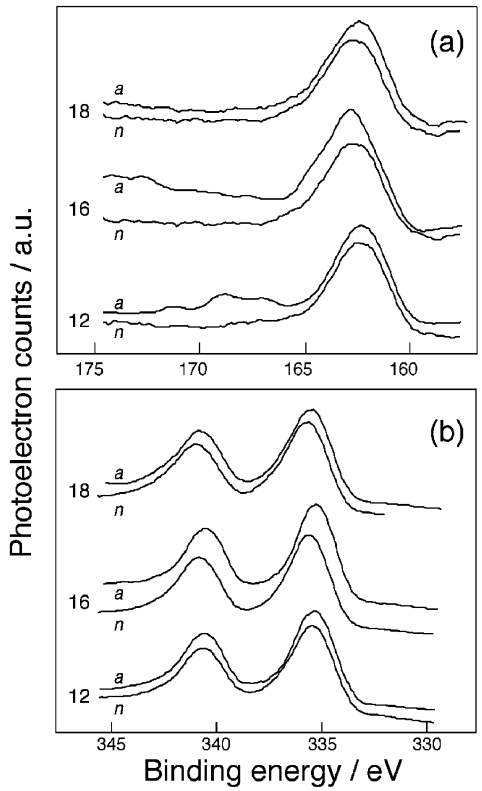

Figure 11. XPS spectra of the Pd:SC_n clusters for the core levels of (a) S(2p) and (b) Pd(3d). The numbers denoted on the curves represent the chain lengths, *n*. The data for the clusters stored for 120 h under air and nitrogen are denoted as "*a*" and "*n*", respectively.

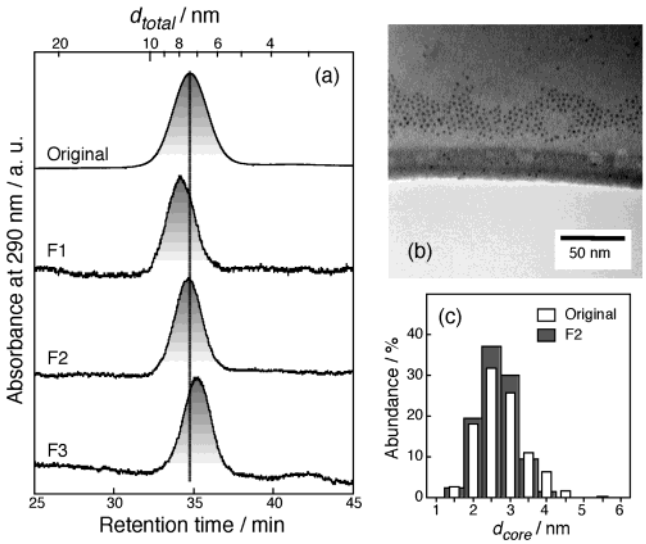

Figure 12. (a) GPC profiles of the Pd:SC_{18} clusters before (top) and after the size selection (F1−F3). (b) TEM image of the clusters in F2, and (c) the core size distributions of the clusters in the original sample and F2.

compared with that of the original sample in Figure 12c. Figure 12c illustrates that the standard deviation for F2 is smaller than that for the original sample. The geometrical parameters of the clusters contained in each fraction are summarized in Table 2. Close inspection of Table 2 reveals the following features: (1) the difference in the d_{total} value is mostly reflected by that in d_{core}; (2) the standard deviations of d_{core} for the fractionated samples are smaller than that of the original sample; (3) the *T* value for each fraction remains to be ca. 2.5 nm regardless of the d_{core}. These findings lead us to conclude that the GPC method is a powerful tool to select the MPCs by the core sizes and to estimate the core sizes of the MPCs from the d_{total} values with a knowledge of the *T* value. Once the *T* values are established, the evaluation of the d_{core} value of the MPCs by the GPC method is superior to that by the TEM observation[32] because the following difficulties are encountered in the later method: it is difficult in the TEM analysis to select objectively the representative area from which the d_{core} values are derived and to measure the d_{core} values precisely from the vague projections of the cores in the TEM micrographs.

TABLE 2: Summary of the Structural Parameters of the Pd:SC_{18} Clusters Fractionated

sample	d_{total}/nm[a]	d_{core}/nm[b]	*T*/nm[c]
original	7.6	2.7 (1.2)	2.5
F1	8.0	3.0 (1.0)	2.5
F2	7.5	2.5 (1.0)	2.5
F3	7.0	2.1 (0.6)	2.5

[a] From Figure 12a. [b] Numbers in parentheses represent standard deviations. [c] Calculated by eq 1.

4. Summary

We have prepared the Pd:SC_n (n = 10, 12, 14, 16, and 18) clusters by the ligand exchange method. The structures and stabilities of the organic layers of the Pd:SC_n clusters are investigated by gel permeation chromatography (GPC) with the help of transmission electron microscopy (TEM), X-ray photoelectron spectroscopy (XPS), and Fourier transform infrared (FT-IR) spectroscopy. The present study reveals that structures and stabilities are heavily dependent on the chain length of the thiolates used to protect the clusters. The main conclusions drawn from the present study are summarized as follows:

(1) The thicknesses of the monolayers can be evaluated from the differences between the hydrodynamic diameters and core diameters of the Pd:SC_n clusters for $n \geq 14$, determined by GPC and TEM, respectively. The thicknesses thus obtained are well reproduced by the length of the thiolates in the all-trans conformations.

(2) The Pd:SC_{18} clusters were fractionated by GPC into a series of the purified samples. The clusters contained in each fraction are not different in the monolayer thicknesses but in their core sizes. Therefore, the core sizes of the clusters can be evaluated by the GPC technique with a knowledge of the monolayer thickness.

(3) The SC_n thiolate monolayers except for n = 18 become disordered spontaneously at room temperature, which accompanies the formation of Pd thiolate complexes. Well-ordered monolayers are reconstructed during the incubation of the clusters in the presence of the free thiols. The reconstruction of well-ordered monolayers by heat treatment may result from the effect of annealing on lateral organization of the thiolates as well as on the Pd core structures.

(4) All of the Pd:SC_n clusters reported here are stable against air oxidation although the monolayers on the Pd clusters contain higher populations of gauche defects than the 2D analogues. The origin of this counterintuitive observation is not clear at present.

The present study illustrates that the GPC serves a sensitive probe for the characterization of the monolayer-protected clusters (MPCs): the retention time gives the total size of the MPC and the transmittance through the columns reflects the degree of structural order in the outermost sphere of the MPC.

Acknowledgment. Professor Takashi Nagata at the University of Tokyo is greatly acknowledged for the critical reading

of the manuscript and fruitful discussions. The authors thank for Professors Toshihiko Yokoyama and Nobuyuki Nishi at IMS for measurements of the XPS and FT-IR spectra, respectively. The present work was supported by a Grant-in-Aid for Creative Scientific Research Collaboratory on Electron Correlations (13NP0201), the 2002th-year Joint Research Project (Soken/K02-1) of Sokendai, and "Nanotechnology Support Project" of Ministry of Education, Culture, Sports, Science and Technology (MEXT), Japan.

References and Notes

(1) Castleman, A. W., Jr.; Bowen, K. H., Jr. *J. Phys. Chem.* **1996**, *100*, 12911.

(2) *Clusters of Atoms and Molecules*; Haberland, H., Ed.; Springer Series in Chemical Physics 52 and 57; Springer: Berlin, 1994.

(3) *Clusters and Colloids*; Schmid, G., Ed., VCH: Weinhiem, 1994.

(4) Brust, M.; Walker, M.; Bethell, D.; Schiffrin, D. J.; Whyman, R. *J. Chem. Soc., Chem. Commun*. **1994**, 801.

(5) Templeton, A. C.; Wuelfing, W. P.; Murray, R. W. *Acc. Chem. Res.* **2000**, *33*, 27.

(6) Whetten, R. L.; Khoury, J. T.; Alvarez, M. M.; Murthy, S.; Vezmar, I.; Wang, Z. L.; Stephens, P. W.; Cleveland, C. L.; Luedtke, W. D.; Landman, U. *Adv. Mater*. **1996**, *8*, 428.

(7) Whetten, R. L.; Shafigullin, M. N.; Khoury, J. T.; Schaaff, T. G.; Vezmar, I.; Alvarez, M. M.; Wilkinson, A. *Acc. Chem. Res.* **1999**, *32*, 397.

(8) Luedtke, W. D.; Landman, U. *J. Phys. Chem. B* **1998**, *102*, 6566.

(9) Garzon, I. L.; Rovira, C.; Michaelian, K.; Beltran, M. R.; Ordejon, P.; Junquera, J.; Sanchez-Portal, D.; Artacho, E.; Soler, J. M. *Phys. Rev. Lett.* **2000**, *85*, 5250.

(10) Dubois, L. H.; Nuzzo, R. G. *Annu. Rev. Phys. Chem.* **1992**, *43*, 437.

(11) Dubois, L. H.; Zegarski, B. R.; Nuzzo, R. G. *J. Chem. Phys*. **1993**, *98*, 678.

(12) Ulman, A. *Chem. Rev*. **1996**, *96*, 1533.

(13) Poirier, G. E. *Chem. Rev*. **1997**, *97*, 1117.

(14) Hostetler, M. J.; Wingate, J. E.; Zhong, C.-J.; Harris, J. E.; Vachet, R. W.; Clark, M. R.; Londono, J. D.; Green, S. J.; Stokes, J. J.; Wignall, G. D.; Glish, G. L.; Porter, M. D.; Evans, N. D.; Murray, R. W. *Langmuir* **1998**, *14*, 17.

(15) Terrill, R. H.; Postlethwaite, T. A.; Chen, C.-H.; Poon, C.-D.; Terzis, A.; Chen, A.; Hutchison, J. E.; Clark, M. R.; Wignall, G.; Londono, J. D.; Superfine, R.; Falvo, M.; Johnson, C. S., Jr.; Samulski, E. T.; Murray, R. W. *J. Am. Chem. Soc.* **1995**, *117*, 12537.

(16) Badia, A.; Gao, W.; Singh, S.; Demers, L.; Cuccia, L.; Reven, L. *Langmuir* **1996**, *12*, 1262.

(17) Badia, A.; Singh, S.; Demers, L.; Cuccia, L.; Brown, G. R.; Lennox, R. B. *Chem. Eur. J.* **1996**, *2*, 359.

(18) Badia, A.; Cuccia, L.; Demers, L.; Morin, F.; Lennox, R. B. *J. Am. Chem. Soc.* **1997**, *119*, 2682.

(19) Andres, R. P.; Bein, T.; Dorogi, M.; Feng, S.; Henderson, J. I.; Kubiak, C. P.; Mahoney, W.; Osifchin, R. G.; Reifenberger, R. *Science* **1996**, *272*, 1323.

(20) Ingram, R. S.; Hostetler, M. J.; Murray, R. W.; Schaaff, T. G.; Khoury, J. T.; Whetten, R. L.; Bigioni, T. P.; Guthrie, D. K.; First, P. N. *J. Am. Chem. Soc.* **1997**, *119*, 9279.

(21) Chen, S.; Ingram, R. S.; Hostetler, M. J.; Pietron, J. J.; Murray, R. W.; Schaaff, T. G.; Khoury, J. T.; Alvarez, M. M.; Whetten, R. L. *Science* **1998**, *280*, 2098.

(22) Simon, U. *Adv. Mater*. **1998**, *10*, 1487.

(23) Chen, S.; Murray, R. W.; Feldberg, S. W. *J. Phys. Chem. B* **1998**, *102*, 9898.

(24) Hicks, J. F.; Templeton, A. C.; Chen. S. W.; Sheran, K. M.; Jasti, R.; Murray, R. W.; Debord, J.; Schaaff, T. G.; Whetten, R. L. *Anal. Chem.* **1999**, *71*, 3703.

(25) Thomas, P. J.; Kulkarni, G. U.; Rao, C. N. R. *J. Phys. Chem. B* **2000**, *104*, 8138.

(26) Reetz, M. T.; Helbig, W.; Quaiser, S. A.; Stimming, U.; Breuer, N.; Vogel, R. *Science* **1995**, *267*, 367.

(27) Yonezawa, T.; Tominaga, T.; Toshima, N. *Langmuir* **1995**, *11*, 4601.

(28) Yonezawa, T.; Tominaga, T.; Richard, D. *J. Chem. Soc., Dalton Trans.* **1996**, 783.

(29) Yonezawa, T.; Toshima, N.; Wakai, C.; Nakahara, M.; Nishinaka, M.; Tominaga, T.; Nomura, H. *Colloids Surf., A* **2000**, *169*, 35.

(30) Toshima, N.; Shiraishi, Y.; Teranishi, T.; Miyake, M.; Tominaga, T.; Watanabe, H.; Brijoux, W.; Bönnemann, H.; Schmid, G. *Appl. Organomet. Chem.* **2001**, *15*, 178.

(31) Wuelfing, W. P.; Templeton, A. C.; Hicks, J. F.; Murray, R. W. *Anal. Chem.* **1999**, *71*, 4069.

(32) Wilcoxon, J. P.; Martin, J. E.; Provencio, P. *Langmuir* **2000**, *16*, 9912.

(33) Wilcoxon, J. P.; Martin, J. E.; Provencio, P. *J. Chem. Phys.* **2001**, *115*, 998.

(34) Wilcoxon, J. P.; Provencio, P. *J. Phys. Chem. B* **2003**, *107*, 12949.

(35) Hostetler, M. J.; Green, S. J.; Stokes, J. J.; Murray, R. W. *J. Am. Chem. Soc.* **1996**, *118*, 4212.

(36) Ingram, R. S.; Hostetler, M. J.; Murray, R. W. *J. Am. Chem. Soc.* **1997**, *119*, 9175.

(37) Hostetler, M. J.; Templeton, A. C.; Murray, R. W. *Langmuir* **1999**, *15*, 3782.

(38) Ionita, P.; Caragheorgheopol, A.; Gilbert, B. C.; Chechik, V. *J. Am. Chem. Soc.* **2002**, *124*, 9048.

(39) Schaaff, T. G.; Whetten, R. L. *J. Phys. Chem. B* **1999**, *103*, 9394.

(40) Chen, S.; Huang, K.; Stearns, J. A. *Chem. Mater*. **2000**, *12*, 540.

(41) Zamborini, F. P.; Gross, S. M.; Murray, R. W. *Langmuir* **2001**, *17*, 481.

(42) Love, J. C.; Wolfe, D. B.; Chabinyc, M. L.; Paul, K. E.; Whitesides, G. M. *J. Am. Chem. Soc*. **2002**, *124*, 1576.

(43) Love, J. C.; Wolfe, D. B.; Haasch, R.; Chabinyc, M. L.; Paul, K. E.; Whitesides, G. M.; Nuzzo, R. G. *J. Am. Chem. Soc*. **2003**, *125*, 2597.

(44) Tsukuda, T.; Kimura, N.; Sasaki, T.; Nagata, T. *Trans. Mater. Res. Soc. Jpn.* **2000**, *25*, 929.

(45) Murayama, H.; Ichikuni, N.; Negishi, Y.; Nagata, T.; Tsukuda, T. *Chem. Phys. Lett.* **2003**, *376*, 26.

(46) Toshima, N.; Harada, M.; Yonezawa, T.; Kushihashi, K.; Asakura, K. *J. Phys. Chem*. **1991**, *95*, 7448.

(47) Toshima, N.; Yonezawa, T.; Kushihashi, K. *J. Chem. Soc., Faraday Trans.* **1993**, *89*, 2537.

(48) Boni, K. A.; Sliemers, F. A.; Stickney, P. B. *J. Polym. Sci.* **1968**, *A-2*, 1579.

(49) Giersig, M.; Mulvaney, P. *Langmuir* **1993**, *9*, 3408.

(50) Martin, J. E.; Wilcoxon, J. P.; Odinek, J.; Provencio, P. *J. Phys. Chem. B* **2002**, *106*, 971.

(51) Porter, M. D.; Bright, T. B.; Allara, D. L.; Chidsey, C. E. D. *J. Am. Chem. Soc.* **1987**, *109*, 3559.

(52) Yee, C. K.; Jordan, R.; Ulman, A.; White, H.; King, A.; Rafailovich, M.; Sokolov, J. *Langmuir* **1999**, *15*, 3486.

(53) Higgins, J. D., III; Suggs, J. W. *Inorg. Chim. Acta* **1988**, *145*, 247.

(54) Li, Y.; Huang, J.; McIver, R. T., Jr.; Hemminger, J. C. *J. Am. Chem. Soc.* **1992**, *114*, 2428.

(55) Horn, A. B.; Russell, D. A.; Shorthouse, L. J.; Simpson, T. R. E. *J. Chem. Soc., Faraday Trans.* **1996**, *92*, 4759.

(56) Scott, J. R.; Baker, L. S.; Everett, W. R.; Wilkins, C. L.; Fritsch, I. *Anal. Chem*. **1997**, *69*, 2636.

(57) Schoenfisch, M. H.; Pemberton, J. E. *J. Am. Chem. Soc*. **1998**, *120*, 4502.

(58) Lee, M.-T.; Hsueh, C.-C.; Freund, M. S.; Ferguson, G. S. *Langmuir* **1998**, *14*, 6419.